Limits on the UV Photodecomposition of Carbonates on Mars

Richard Quinn[1]

Aaron P. Zent[2]

and

Christopher P. McKay[2]

[1]SETI Institute, NASA Ames Research Center

Mail Stop 239-12, Moffett Field, CA 94039

[2] NASA Ames Research Center

Mail Stop 245-3, Moffett Field, CA 94039

Pages: 41, Figures: 4, Tables: 1

Running Head: Limits on the Photodecomposition of Carbonates on Mars

Corresponding Author: Richard Quinn, NASA Ames Research Center, Mail Stop 239-12

Moffett Field, CA 94039

rquinn@mail.arc.nasa.gov

Abstract

The effect of UV light on the stability of calcium carbonate in a simulated martian atmosphere was experimentally investigated. Sample cells containing ^{13}C labeled calcite were irradiated with a Xe arc lamp in 10 mbar of simulated martian atmosphere and a quadrupole mass spectrometer was used to monitor the headspace gases for the production of $^{13}CO_2$. We found no experimental evidence of the UV photodecomposition of calcium carbonate in a simulated martian atmosphere. Extrapolating the lower limit of detection of our experimental system to an upper limit of carbonate decomposition on Mars yields a quantum efficiency of 3.5×10^{-8} molecules/photon over the wavelength interval of 190-390 nm and a maximum UV photodecomposition rate of 1.2×10^{-13} kg m^{-2} s^{-1} from a calcite surface. The maximum loss of bulk calcite due to this process would be 2.5 nm yr^{-1}. However, calcite is expected to be thermodynamically stable on the surface of Mars and potential UV photodecomposition reaction mechanisms indicate that while calcium carbonate may decompose under vacuum, it would be stable in a CO_2 atmosphere. Given the expected stability of carbonate on Mars and our inability to detect carbonate decomposition, we conclude that it is unlikely that the apparent absence of carbonate on the martian surface is due to UV photodecomposition of calcite in the current environment.

Keywords: Mars, surface; Photochemistry; Geochemistry; Mineralogy; Exobiology

1. Introduction

Martian carbonate deposits are thought to hold the key to unraveling the nature of the Noachian climate. The inability to detect martian carbonates has surprised many workers, and led to a number of hypotheses for their absence. We discuss the UV-photodecomposition hypothesis below, and our attempts to experimentally verify it.

1.1 Identification of carbonates on Mars

Data from Earth-based spectra, Mariner 6/7, and the SNC meteorites ambivalently indicate that carbonates may be present on the surface of Mars. Clark et al. (1990) attributed their observation of adsorption features near 2.3 μm to the presence of carbonate, bicarbonate, and bisulfate in the mineral scapolite. Blaney and McCord (1990) placed an upper limit of 3-5% on the carbonate content of the surface based on the lack of carbonate adsorptions bands in the 3-4 μm spectral region. Studies by Pollack et al. (1990) of bands near 6.7 and 7.3 μm were used to infer a coating of 1-3% carbonate on the airborne dust. In all cases, bands observed in earth-based spectra attributed to carbonate are weak and the identification of carbonates is not conclusive.

Roush et al. (1986) and McKay and Nedell (1988) unsuccessfully searched selected portions of Mariner 6/7 infrared spectrometer data for carbonate features. McKay and Nedell (1988) pointed out, however, that the data do not cover the locations that are most likely to be formed of carbonates, such as the layered sediments in the Valles Marineris.

In their review of the lack of spectral evidence for carbonates, Calvin et al. (1994) suggested that if hydrous carbonates were present, they would not be as prominent spectrally and could therefore be present on the surface in considerable amounts without being spectrally detectable. Calvin et al. (1994) observed that, in the presence of H_2O and CO_2, hydrous carbonates can form without liquid water as weathering products of mafic materials at subfreezing temperatures. They suggest that hydrous carbonate may be present metastably in the current martian environment because kinetic factors may prevent dehydration.

Carbonates have been observed in the SNC meteorites from Mars as well as ALH84001 (e.g. Gooding et al. 1992; Write et al. 1992; Jull et al. 1995). The presence of carbonates does imply that they are a stable weathering product in the subsurface environment that yielded the SNC meteorites (Gooding et al. 1992). However, in all cases carbonates form minor inclusions.

Mars has been mapped at 3 x 6 km resolution by the Thermal Emission Spectrometer on the Mars Global Surveyor and no evidence of carbonates has been found. Kirkland et al. (2001) have determined detection limits for carbonates using a linear deconvolution method; they claim that the limit for carbonates would be about 10%. This detection limit would amount to the detection of an outcrop on the order of 2 km^2, or a 3x6 km region of the planet containing at least 10% carbonate.

1.2 Formation of carbonates on Mars

As has been discussed extensively in the literature, it is thought that Mars once had a thick CO_2 atmosphere, which is now in the form of carbonate deposits. There are two lines of evidence that suggest that Mars had a thicker atmosphere during the Noachian epoch (3.8 Gyr ago). First is the evidence of much higher erosion rates in the Noachian terrain compared to younger terrains. Carr (1992) has estimated that the erosion rate on Noachian surfaces was 2-10 $\mu m\ yr^{-1}$, a value comparable to the low end of terrestrial erosion rates. Post-Noachian erosion rates are on the order of 0.02 $\mu m\ yr^{-1}$ ($2x10^{-8}$ m yr^{-1}). The second line of evidence is the presence of fluvial channels on the Noachian surface, indicating a stable flow of liquid water.

Both of these lines of evidence suggest that Mars had a thicker, warmer atmosphere at the end of the Noachian than it does today. Paradoxically, these warmer conditions existed when the solar luminosity was about 0.8 of its present value. For many years, it was generally believed that a several-bar atmosphere of CO_2 would provide an adequate greenhouse effect to allow for surface conditions consistent with a hydrological cycle and the concomitant fluvial and erosion features (e.g. Pollack et al. 1987; Fanale et al. 1991). However, over time the thick CO_2 atmosphere would be removed through the precipitation of carbonate resulting from the formation of CO_3^{-2} by dissolved CO_2 and the dissolution of Ca^{+2} from silicate rocks. The formation of carbonate would result in a net loss of CO_2 from the atmosphere, which would continue until the atmospheric pressure approached the triple point of water and liquid water was no longer formed (Kahn 1985).

Theoretical models suggest that carbonate formation would proceed for 10 to 100 million years before the thick CO_2 atmosphere would be reduced to current surface pressures (Pollack et al. 1987; McKay and Davis 1991; Haberle et al. 1994). Recycling of carbonate has been suggested as the mechanism by which a thick atmosphere was maintained during the Noachian; Pollack et al. (1987) and Schaefer (1990) suggested volcanic recycling, while Carr (1989) suggested impact recycling. The drop-off of recycling due to lower heat flow or the cessation of impacts would account for the drop in atmospheric pressure and the lowering of temperatures at the end of the Noachian. Without plate tectonics to subduct carbonate sediments and thereby decompose them to CO_2, Mars had no mechanism to recycle carbonates and the planet quickly cooled to its current state.

Along these lines, Griffith and Shock (1995) have suggested that rainfall is not necessary to form carbonates and that hydrothermal systems could have formed massive subsurface carbonate deposits. Nonetheless, when these systems reached the local surface, carbonate precipitation would have covered the surface with exposed carbonates.

The entire thick CO_2 hypothesis was thrown into question when Kasting (1991) pointed out that a thick CO_2 atmosphere on early Mars would not be able to warm the surface sufficiently to allow for water to flow, due to the condensation of the atmospheric CO_2. To warm Mars to a globally averaged temperature of 273 K early in its history, when the solar luminosity was 0.8 times its present value, requires an atmospheric pressure of about 3-5 bars of CO_2 (Pollack et al. 1987). However, at these high levels the partial pressure of CO_2 in the upper atmosphere exceeds its saturation point. The resulting condensation changes the temperature lapse rate, with the net effect of cooling the

planet's surface. Hence, there is a limit to the amount of greenhouse warming that is possible with a CO_2 and H_2O atmosphere. This effect had been previously noted by Gierasch and Toon (1973) but was not properly incorporated into greenhouse models of Mars until 1991. Thus theoretical models imply that the CO_2 greenhouse could not warm Mars to temperatures above -50°C early in its history. Unless they invoke greenhouse gases other than CO_2, such as CH_4, current climate models cannot adequately explain the hypothesized surface conditions on Mars during the Noachian or the existence of channels on younger terrain. However, recent models which include the effects of clouds (Forget and Pierrehumbert, 1997; Mischna et al. 2000) show that carbon dioxide clouds could result in a net warming and generate surface temperatures near freezing.

1.3 The effect of UV light on carbonate formation and stability

The lack of unambiguous spectral evidence for carbonates on Mars has led to the suggestion that they may be unstable on the Martian surface. Mukhin et al. (1996) have conducted experiments in which natural calcite crystal (99.94%) was exposed under vacuum to UV light. They reported a mean quantum yield for the photo-induced release of CO_2 of 10^{-5} molecules per photon over a wavelength interval of 190-390nm and a threshold effect at 350-400 nm; longer wavelength photons were not reported to decompose carbonates.

This is a surprising result to us because of the high threshold effect reported and because previous work (Booth and Kieffer 1978) had shown that carbonates form under conditions similar to those on Mars even with UV light present. Additionally, the Mukhin

et al. (1996) results may not be applicable to Mars due to the unrealistically low partial pressure of CO_2 (10^{-8} mbar) in their system.

We have experimentally investigated the photo-induced decomposition of calcium carbonate in a simulated Martian atmosphere (at a pressure of 10 mbar). Because the stability of carbonates on the surface of Mars may differ from that of carbonate samples exposed to UV light at high temperatures and/or under vacuum, a series of experiments was carried out to investigate the temperature dependence of UV-induced carbonate decomposition in a simulated Mars atmosphere.

2. Experimental

2.1 Experimental apparatus

Experiments were carried out in ultrahigh-vacuum-compatible 34.5 cc stainless steel reaction cells. Each cell utilized a stainless steel bellows valve for introduction and extraction of headspace gases, and a 2.54 cm sapphire view port for illumination of samples. All seals were conflat-type metal compression seals, ensuring a leak-tight system. An ultrahigh-vacuum-compatible cell system was used in order to provide a low cell pressure (~10^{-8} mbar) during sample bake-out and to ensure insignificant leak rates into the cell during UV exposures. The experimental setup used for UV exposures is shown in Fig. 1. After preparing a sample (described in section 2.2), the cell was fitted into an aluminum cold-block which was temperature controlled using a FTS Systems recirculating cooler with a lower temperature limit of 173K. A Photon Technologies

International 150-watt Xe arc lamp with an ellipsoid reflector was used to illuminate the samples. A 18 cm water filter cooled with recirculating water was used to prevent IR heating of the samples during illumination. The entire system (lamp, filter, cell, and cold block) was enclosed in a glove bag purged with dry nitrogen to prevent condensation of water ice on the surface of the cell windows during illumination and to minimize UV adsorption by gases in the optical path between the lamp and sample cell.

2.2 Sample preparation

99.6% purity labeled calcium carbonate, 99.1% ^{13}C, (Isotec Inc.) was used to allow carbonate decomposition to be differentiated from the CO_2 present in the simulated Mars atmosphere used in the experiments (CO_2 97.27%, N_2 2.7%, O_2 0.13%). The samples were identified to be calcite by X-ray diffraction analysis (Micron Inc.). 0.5-gram samples of the $^{13}CaCO_3$ were placed in planchets and lightly pressed to yield a flat and uniform surface area. Two different types of planchets were used, Pyrex glass (1.3 cm^2) and aluminum (7.9 cm^2). The planchets containing the samples were placed on the bottom of the stainless steel cells and a knife-edge compression seal on the cell was made using an annealed copper gasket. Once sealed, the cells were attached to a turbo-pumped high-vacuum system with an oil-free diaphragm foreline pump (base pressure 10^{-8} torr) and baked out under vacuum to remove adsorbed gases and surface contaminants. Gases desorbed during sample bake-out were monitored using a Stanford Research Systems Residual Gas Analyzer (quadrupole mass spectrometer).

After sample bake-out, the sample cells were filled to 10 mbar with a simulated martian atmosphere gas mixture consisting of 97.27% CO_2, 2.7% N_2, and 0.13% O_2 (AirGas Inc).

2.3 Experimental Procedure

Once prepared, the sample cells were placed in the temperature-controlled aluminum cold block and, after purging the glove bag with dry nitrogen, the cell was allowed to cool. Temperature was monitored with k-type thermocouples mounted in three locations: in the aluminum block, in the lower wall of the stainless steel sample cell, and directly above the sapphire view port outside the sample cell. The temperature of the sample was not measured directly. Experiments were run for periods of up to 70 hours at four cell temperatures: 423K, 323K, 278K, and 243K. In each experiment the lamp was positioned to provide a UV flux of no more than ~10^{17} photons $cm^{-2}s^{-1}$, since a linear dependence of photo-decomposition rate on light intensity up to this flux was observed by Mukhin et al. (1996). After the UV exposure period was completed, the cells were allowed to warm to room temperature and then analyzed using the RGA backed with a Varian turbomolecular pump with an oil-free diaphragm foreline pump. Samples of headspace gases were admitted into the RGA through a leak valve. Production of $^{13}CO_2$ was monitored by analyzing changes in 45/44 ($^{12}CO_2^+$)/($^{13}CO_2^+$) mass ratio.

2.4 Calibrations

2.4.1. UV lamp calibrations The Photon Technologies International UV lamp with a 150-watt Xe short arc lamp (Ushio Inc.) was calibrated using an Ultra Violet Products (UVP) radiometer and sensors calibrated with standards traceable to the National Physics Laboratory (UK). Calibration measurements were taken using UVP narrow band sensors with the sapphire window in place over the calibration sensors. The flux at the peak transmission for each of the sensors (254nm, 295nm, 365nm, and 405nm) was determined utilizing spectral bandpass data provided with each of the calibrated sensors. The total UV flux each sample received was determined by integrating the UV portion of the four-point calibration curve. A comparison of the calibrated spectrum of the Xe lamp to the UV flux at the surface of Mars (Khun and Atreya, 1979) is shown in Fig. 2.

2.4.2.Mass Spectrometer Calibrations The RGA used for analyzing the sample headspace gases was calibrated using 99.9% purity ^{13}C labeled CO_2 (Isotec Inc.). The total ^{13}C content in the standard gas equaled 99.1 atom % and ^{12}C content equaled 0.9 atom %. Ar/O_2 and N_2 contamination was less than 50 ppm, CO contamination less than 20 ppm, and total hydrocarbon content less than 20 ppm. Calibration standards were produced by introducing a small amount of $^{13}CO_2$ gas into empty sample cells that had been pumped to $\sim 10^{-8}$ mbar. The pressure of the $^{13}CO_2$ standard gas in the cells was measured using a Baratron™ capacitance manometer. After introduction of the $^{13}CO_2$ calibration standard, each cell was back-filled with the simulated Mars atmosphere mixture to raise the total pressure of the cell to ~10 mbar. Calibration curves were created by plotting the $(^{13}CO_2^+)/(^{12}CO_2^+)$ mass ratio (45/44) against the pressure of $^{13}CO_2$ that was added to the cells. The standards were introduced into the RGA system through a leak valve in the same manner as for sample analysis. For each experiment, three

background measurements were taken of simulated Mars atmosphere mixture without added $^{13}CO_2$. The standard deviation of these background measurements was used to determine the lower limit of detection (LLD = 2σ) for each experiment. A linear detector response was observed over the range of 0 to 0.2 mbar (0 to 1.7×10^{17} molecules) of $^{13}CO_2$ added to the sample cells. A representative calibration curve is shown in Fig. 3.

3. Results

A summary of run conditions and results is given in Table I. The baseline and standard deviation for an experimental set were determined by repeat injections of Mars gas without added $^{13}CO_2$ standard. In some runs (A1 and A3) the measured 45/44 mass ratio was greater than the lower limit of detection (LLD), which was taken to be two times the standard deviation of the baseline 45/44 mass ratio for that run. In the case of run A1, the run showing the largest 45/44 mass ratio above the LLD, a quantum yield for carbonate decomposition can be calculated to be 3×10^{-7} molecules/photon. For all runs, the flux used to calculate either the quantum yield (run A1) or the LLD was determined from the run calibration curve for wavelengths below 390 nm. This wavelength was chosen to facilitate comparison with the Mukhin et al. (1996) work. Although Mukhin et al. (1996) reported a threshold effect at 350-400 nm for the decomposition of carbonate under vacuum, in drawing their conclusions and extrapolating their experimental results to Mars, Mukhin et al. (1996) used 390 nm for the long-wavelength cut-off and considered 10^{-5} molecules/photon to be the mean quantum yield over the wavelength interval of 190-390 nm. For reasons discussed below, even if UV decomposition of

carbonate is taking place, the cut-off is probably shortward of 390 nm; photoactivity out to 390 nm would imply that carbonates are also being photodecomposed on earth. Our calculated quantum yield of $3x10^{-7}$ molecules/photon for run A1 compares to the mean yield of $\sim 10^{-5}$ for incoming photons between 190 and 390 nm nm reported by Mukhin et al. (1996).

Although the 45/44 mass ratio in run A1 exceeded the LLD, thereby permitting the calculation of a quantum efficiency, we attribute the production of $^{13}CO_2$ in experiments A1 or A3 not to UV decomposition but to a thermal release of adsorbed or trapped $^{13}CO_2$ from the carbonate sample. To analyze this thermal effect, it is useful to divide the experiment runs into two sets based on sample pre-run treatment. Although all samples were pumped down overnight to the 10^{-8} mbar range, each was subjected to a different thermal treatment during the pump-down procedure. As Table I shows, three irradiated samples (A1, A2, and A3) and a blank run (consisting of a non-illuminated sample cell containing $Ca^{13}CO_3$ and Mars gas mixture) were held at room temperature during the pump-down, while the four other samples (A4, B1, B2, B3) were baked out during pump-down. Other than run A1, only runs A3 and the blank run had measured 45/44 mass ratios that exceeded two standard deviations of the baseline. The run temperatures of samples A1 and A3 exceeded the bake-out temperature, while the blank was held at room temperature and not subjected to UV exposure. Another sample held at room temperature during pump-down, A2, had a 45/44 ratio of less than one sigma; however, it was held at subambient temperatures (i.e. it did not exceed its bake-out temperature) during the course of the experiment. In samples that were not baked out, $^{13}CO_2$ was released (or

possibly exchanged with the headspace $^{12}CO_2$) even if the sample was not exposed to UV radiation, unless the sample was cooled during the experiment.

These results can be compared to the samples that received high-temperature bake-out during sample pump-down. Samples B1 and B2 were each baked out at 490K, while samples B3 and A4 were baked out at 625K and 675K respectively. In three of these cases (B1, B2, B3), the samples were held slightly below room temperature (~278K) during UV illumination. In all three cases the measured 45/44 ratios after illumination were less than one standard deviation of the baseline. The fourth sample, A4, which was heating during pump-down, was heated during UV illumination to a temperature of 325K, substantially below its bake-out temperature of 675K. Again, in this case, as with the other samples that were baked out, the post-illumination 45/44 ratio was less than one standard deviation above the baseline. In summary, we see no evidence for the UV decomposition of $CaCO_3$ in our experiments. Nevertheless, we cannot, of course, rule out that the reaction may be occurring at a rate below our LLD. However, as can be seen in Table I, even if this were the case, the upper limit of the quantum efficiency with which the UV decomposition of carbonate can take place is ~$3x10^{-8}$ molecules/photon, more than 2.5 orders of magnitude lower than the 10^{-5} quantum efficiency reported by Mukhin et al. (1996) for the UV decomposition of $CaCO_3$ measured under vacuum.

4. Discussion

Our inability to detect the photodecomposition of carbonate in our experimental runs leads to two possible conclusions: that decomposition does not take place in a Mars atmosphere, or that decomposition is taking place with a quantum efficiency below $3.5x10^{-8}$ molecules/photon. Below we consider these two possibilities, examine why we expect carbonates to be stable on the surface of Mars, suggest possible mechanisms for the UV decomposition of carbonates, and discuss implications of carbonate UV-decomposition rates below $3.5x10^{-8}$ molecules/photon on the surface of Mars.

4.1 Thermodynamic effects of CO_2 Partial Pressure

The stability of carbonates on Mars has been the subject of considerable research (e.g. O'Connor, 1968; Gooding, 1978; Fegley and Treiman, 1992) that has yielded a detailed set of chemical equilibrium equations that can be solved for the stability fields of carbonates. Each of these studies concluded that not only are carbonates thermodynamically stable at the current CO_2 surface pressures on Mars, but that virtually all the available CO_2 should eventually be converted to carbonates.

Thermodynamically, the work of Muhkin et al. (1996) and the role of system CO_2 pressure can be examined by considering the heterogeneous formation (solid-gas) of carbonates on Mars in the absence of water. Although the case presented is simplified, it is applicable to the experiments of Mukhin et al. (1996). However, it does not accurately represent the work of Booth and Kieffer (1978), who included thermodynamically significant levels of water in their experimental system. Nonetheless, it illustrates the important role of CO_2 partial pressure on carbonate stability.

The heterogeneous decomposition of calcite can be represented by the reaction

$$CaCO_3 \rightarrow CaO + CO_2 + \Delta G_T^o \qquad (1)$$

where G^o is the Gibbs free energy of the reaction, which is a function of temperature (the Helmholz free energy defined for constant volume reactions). At low temperatures G^o is positive (130 kJ at 25°C), indicating that calcite is quite stable. However, at elevated temperatures G^o becomes negative and calcite decomposition proceeds with the formation of CaO according to Eq. 1.

The Gibbs free energy of the reaction is given by

$$\Delta G = \Delta H - T\Delta S \qquad (2)$$

where ΔH is the enthalpy of formation and ΔS is the entropy. As temperature increases, the second term in Eq. 2 (TΔS) increases due to its explicit temperature dependence and because one of the reaction products, CO_2, is in the gas phase and the entropy is approximately linearly proportional to temperature. Thus, because ΔH is roughly temperature independent, as temperature increases the second term becomes dominant and eventually ΔG^o becomes negative.

A low and constant CO_2 partial pressure is implicit in the above discussion. (Strictly speaking, it is the fugacity that is low and constant, but for all conditions considered here, the fugacity is equal to the partial pressure to adequate accuracy). Of course, in a closed system calcite decomposition would result in the generation of CO_2 until equilibrium is

reached, with the back reaction of Eq. 1 proceeding at the same rate as the forward reaction. Assuming that the activity coefficients of $CaCO_3$ and CaO are unity (as pure solids), the equilibrium partial pressure of CO_2 is given by

$$p^eCO_2 = \exp[-\Delta G°/RT] \tag{3}$$

where R is the universal gas constant. When the system partial pressure of CO_2 is not equal to its equilibrium value, a free energy difference is generated which drives the reaction toward the direction that will establish equilibrium. The value of this free energy is given by

$$\Delta G° = -RT \ln[pCO_2/p^eCO_2]. \tag{4}$$

At room temperature, $\Delta G°$ for the decomposition of carbonate is approximately 130 kJ $mole^{-1}$ (Stern and Weiss 1969), so the expected equilibrium CO_2 partial pressure for the experiments carried out at room temperature in this work and for the experiments carried out by Mukhin et al. (1996) is approximately 10^{-23} bar. In both cases, the actual CO_2 partial pressure greatly exceeded this value, which should drive the reaction toward the formation of carbonate with the value of $\Delta G°$ reduced by an amount given by Eq. 4. This value is equal to -120 kJ $mole^{-1}$ ($pCO_2 \sim 10$ mbar) in this work and -68 kJ $mole^{-1}$ ($pCO_2 \sim 10^{-8}$ mbar) in the Mukhin et al. (1996) work. There is considerably more (almost double) free energy driving the formation of carbonates, and resisting their decomposition, under

the realistic P_{CO2} experimental conditions in this work than under the vacuum conditions of the Mukhin et al. (1996) work.

It is interesting to compare these free energy values with the activation energy reported for carbonate decomposition. Stern and Weise (1969) surveyed reported values of the activation energy and found that nearly all are approximately 167 kJ $mole^{-1}$. Thus, the energy of back reaction (formation of carbonates) in this work is comparable to the activation energy, while in the Mukhin et al. (1996) work it is considerably less. This discrepancy might explain the difference between our results; higher CO_2 partial pressure may inhibit photodecomposition of the carbonates.

It should be mentioned that both our experiments and those of Mukhin et al. (1996) examined only the possibility of carbonate decomposition and not the reverse reaction. Booth and Kieffer (1978), in a carefully conducted study, demonstrated the growth of carbonates on rock powder exposed to UV in the presence of CO_2 ranging from 100 to 500 mb. Another of their findings relevant to the discussion here is that the carbonate formation rate was proportional to the pressure of CO_2 over the range of 100 to 500 mb.

4.2 Effects of UV light

However intriguing the thermodynamic discussion given above, it is an incomplete description in that it does not include the effects of UV light. On Mars, absorption by CO_2 effectively blocks penetration of solar radiation below 200 nm. On Earth, O_2 and O_3 block radiation below 300 nm. Therefore the 200-300 nm region (roughly the UVB) reaches the surface of Mars but not the surface of Earth. This spectral region has

important biological effects because the photons in this spectral region have sufficient energy to damage chemical bonds. The energy of a 200 nm photons is 600 kJ per mole. An important point to consider is that the number of solar photons drops rapidly with decreasing wavelength; for example, at the top of the Earth's atmosphere the number of photons at 300 nm is approximately 10^{14} photon cm^{-2} s^{-1} nm^{-1} while at 200 nm the value is approximately 10^{11} photon cm^{-2} s^{-1} nm^{-1}. Thus, longer wavelength photons will dominate any reaction that is activated by photons with wavelengths below 350-400 nm, such as the decomposition of $CaCO_3$, as suggested by Mukhin et al. (1996). Such reactions should occur on both Earth and Mars, at essentially the same rate, since the rate will be dominated by the longest wavelength capable of affecting the reaction.
On Earth there are obviously long-lived surface deposits of carbonate. For example, the Guadalupe Mountains in Texas are the subareal extent of a Permian-age carbonate reef. If Mukhin et al. (1996) are correct, then these carbonates are slowly decomposing due to exposure to 300-350 nm radiation reaching the surface of the Earth.

How, then, can one reconcile the upper limit on the quantum efficiency of carbonate decomposition on Mars of $\sim 10^{-8}$ established in this work (along with the apparent UV-stability of carbonate deposits on Earth) with the 10^{-5} quantum yield reported by Mukhin et al. (1996)? Numerous studies have examined the generation of defects in carbonates by irradiation, e.g. Stoesser et al. (1996), Bartoll et al. (2000). These works are primarily concerned with radiation defects in relation to Electron Spin Resonance (ESR) spectroscopy dating. Most of these works examined the generation of defects by high-energy γ radiation; very few studies addressed the effects of UV light on the structure of calcium carbonate. In fact, we were able to find in the literature only one study that

reported the generation of electronic defects in calcium carbonate by UV light (Bartoll et al. (2000).

As is the case with studies of the effects of high-energy irradiation of carbonates, Bartoll et al. (2000) examined the effects of UV/VIS light on carbonates in relation to ESR dating techniques. They found that radical species such as CO_2^- and CO_3^- could be generated by exposing synthetic and natural calcium carbonates to sunlight or a Hg (Xe) lamp. They also found that while these and other radical species normally observed in carbonates exposed to high energy radiation (α,β,γ) can be generated by exposure to lower-energy UV light, there are numerous subsequent reactions that take place, such as recombination and conversion into other centers. Bartoll et al. (2000) also found that the presence of manganese, iron, or zinc in the carbonate can serve as a sensitizer for the formation of radicals while at the same time causing optical bleaching of defects. Therefore, it is possible that in the Mukhin et al. (1996) work, UV irradiation resulted in the generation of electronic defects, including possible CO_2^-, and CO_3^- radicals, and that these species subsequently formed CO_2 gas. However, several thermal, mechanical, and optical pathways exist through which photo-generated centers can recombine, convert, or be bleached, and although Bartoll et al. (2000) documented the bleaching and conversion of defects in calcium carbonate by UV light, they did not report the generation of CO_2 from any of the observed centers. They also did not specify whether there were any background gases present during the UV exposure. If in fact the exposure was carried out in air, or if trace amounts of O_2 or CO_2 were present, CO_3^- could be formed through the generation of radicals from adsorbed O_2 and CO_2

$$O_{2\ adsorbed} + h\nu \rightarrow 2O^{-} \quad (5)$$

$$CO_{2\ adsorbed} + O^{-} \rightarrow CO_3^{-} \quad (6)$$

If CO_3^{-} radicals are formed on calcium carbonate by UV radiation, either by radical formation on the surface due to adsorbed gas or by defect formation in the lattice, there are several mechanisms by which these centers can recombine, convert, or react (especially if headspace gases are present). One probable mechanism that can result in the formation of CO_2 gas is photodetachment and photodissociation of the CO_3^{-} radical:

$$CO_3^{-} + h\nu \rightarrow CO_2 + O^{-} \quad (7)$$

This reaction has been studied extensively in the gas phase in the context of negative ion chemistry in the ionosphere (Moseley et al. 1974, Hiller and Vestal 1980, Hunton et al. 1984). Mosely et al. (1974) reported that photodetachment thresholds for CO_3^{-} are above 3eV while photodissociation occurs between 2.35 and 2.71 eV. In these works, it has been found that when the reaction 7 is carried out at high CO_2 pressures, the O^{-} produced from the photodissociation undergoes recombination with CO_2 gas to reform CO_3^{-}.

$$2CO_2 + O^{-} \rightarrow CO_3^{-} + CO_2 \quad (8)$$

In these studies the rate of recombination is dependent on both the CO_2 pressure and the time the CO_3^- resides in the drift tube in which it is generated. As drift time increases, CO_2 pressure must decrease to prevent O^- from reacting with CO_2 to reform CO_3^-. Typically, the CO_2 pressure in the drift tube is kept below 0.1 torr to minimize conversion of CO_2 back into CO_3^- as the CO_3^- exits the drift tube.

In the case where the CO_3^- radical is generated as a surface defect on the carbonate crystal, reaction 7 can proceed at a rate limited by the rate of removal of CO_3^- from the surface through the formation of CO_2. When the reaction take places at low CO_2 pressures, as was the case in the Mukhin work, the reaction 7 proceeds in the forward direction as written and results in the release of CO_2 gas from the carbonate surface. When the system CO_2 pressure is high, as was the case in this work (10 mbar), a steady state between reactions 7 and 8 can be established with no net production of CO_2. Because there is a finite number of CO_3^- centers that may form on the surface of the carbonate crystal, in our work the formation of $^{13}CO_2$ would be limited to the maximum number density of CO_3^- centers that can be formed on the crystal. After the initial formation of $^{13}CO_3^-$ sites and subsequent formation of $^{13}CO_2$, the centers will reform through

$$2\ {}^{12}CO_2 + O^-_{\text{surface}} \rightarrow {}^{12}CO_{3\ \text{surface}}^- + {}^{12}CO_2 \qquad (9)$$

suppressing the generation of new $^{13}CO_2$ centers and halting the generation of $^{13}CO_2$ at a level below the LLD. Likewise, on Mars the decomposition of calcite crystal would be suppressed by the maintenance of surface defect populations through reaction 8.

4.3 UV decomposition at rates below $3x10^{-8}$

Although there was no experimental evidence for UV-induced carbonate decomposition using baked-out samples or in samples that were held at low run temperatures, it is possible that decomposition occurred at a rate below the experimental detection limit. This limit can be used for comparison to the Mukhin et al. (1996) work and to determine an upper limit for possible UV-induced carbonate decomposition on Mars. Extrapolating their results to Mars, Mukhin et al. (1996) utilized a value of $2x10^{15}$ photons $cm^{-2}s^{-1}$ for the flux of photons at the surface over the wavelength interval of 190-390 nm. Based on carbonate abundances of 0.01 to 1% in the martian regolith and their measured mean quantum yield of 10^{-5} molecules/photon, Mukhin et al. (1996) predict a CO_2 flux into the atmosphere of 10^{-8} to 10^{-6} molecules $cm^{-2}s^{-1}$ and suggest that this process is a net source of CO_2 to the atmosphere. They assert that the photodecomposition of carbonates could deliver ~10^{23} to 10^{25} molecules cm^{-2} of CO_2 to the martian atmosphere over 4 x 10^9 yr, a yield equivalent to that of the decomposition of a carbonate layer several hundred meters thick (Mukhin et al. 1996).

Stocker and Bullock (1997) examined the photodecomposition of glycine in a simulated martian atmosphere and determined the quantum efficiency of the reaction over the range of 200 to 240nm to be $1.46x10^{-6}$ molecules/photon, an order of magnitude

lower than the quantum efficiency of 10^{-5} reported by Mukhin et al. (1996). Taken together, these are surprising results since they indicate that the carbonates on the surface of Mars are more readily destroyed by UV light than are organic compounds. In contrast, the upper limit for the photodecomposition of carbonates on Mars established in this work is 3.5×10^{-8} molecules/photon, indicating that if photodecomposition of carbonates is occurring on Mars, the carbonates are considerably more stable than organic compounds. Using 3.5×10^{-8} for the quantum efficiency of carbonate decomposition and the same value of UV photon flux at the surface of Mars used by Mukhin et al. (1996) (2×10^{15} photons cm^{-2} s^{-1}), the upper limit of carbonate decomposition from bulk calcite (unmixed in the martian regolith) would be 1.2×10^{-13} kg m^{-2} s^{-1}, which corresponds to a maximum rate of photo-induced chemical weathering of 2.5 nm yr^{-1} (2.5×10^{-9} m yr^{-1}, eight times less than the estimate of mechanical erosion/deposition by Carr (1992)). Over geological time scales (4×10^{9} Gyr), this would be equivalent to the decomposition of 10 meters of a pure calcium carbonate outcrop, assuming that the reaction doesn't cease due to expected passivation of the carbonate surface.

An erosion rate of 0.02μm (Carr, 1992) would erode bulk carbonate outcrops and mix them with the regolith material faster than the outcrops could photodecompose. This abrasion and mixing would lead to the dilution of carbonates in the regolith and the covering of carbonate outcrops by wind-borne sedimentation, resulting in an attenuation of the UV flux to which carbonate would be exposed and a decrease in the net rate of carbonate decomposition per unit surface area. Once mixed with the regolith material, in the absence of continued erosion and mechanical mixing of the regolith, photodecomposition would be limited to the photon penetration depth in the regolith, and

decomposition of exposed carbonate surfaces would be expected to cease due to passivation. Therefore, any photodecomposition of carbonate would be limited by surface abrasion rates, the rate at which abrasion exposes fresh reaction surfaces, and the rate at which unreacted carbonate is cycled to the surface.

Although the rate at which the martian surface material is eroded and mechanically mixed is unknown, we can examine relative rates of erosion, mechanical mixing, and photodecomposition to assess the implications of potential low-rate loss of carbonate on the surface due to photodecomposition. For the purposes of this discussion, we restrict the use of the term "erosion" to the carbonate outcrops, and use the term "deflation" to refer to stripping and removal of particulate material from the regolith. "Deposition" is assumed to be equal on both outcrops and regolith. The combined effects of deflation and deposition over many years results in "mixing" the regolith to some depth. Photodecomposition operates with equal quantum efficiency on both bulk carbonate outcrops, and on carbonate clasts in the regolith.

The first scenario is the photodecomposition of carbonate under conditions of low regolith mixing and erosion rates greater than 2.5 nm yr^{-1}. In this case, the rate at which a carbonate outcrop is eroded and carbonate fragments subsequently diluted and buried in the regolith would exceed the photodecomposition loss rates and result in the accumulation of carbonate in the soil. For example, a post-Noachian erosion rate of 0.02 $\mu m\ yr^{-1}$ (Carr, 1992) would yield a carbonate sedimentation rate of 1.6×10^{-6} kg m^{-2} yr^{-1}, assuming that 3% of the eroded surface material is carbonate. Taking into account a maximum photodecomposition rate of carbonate of 2.0×10^{-7} kg m^{-2} yr^{-1}, (based on a 3% carbonate component in the soil and a photodecomposition quantum efficiency of $3.5 \times 10^{-}$

^{8}), the result is a net accumulation of 1.4×10^{-6} kg m^{-2} yr^{-1} of carbonate in the regolith as the unreacted carbonate is buried by freshly eroded surface material.

In the second scenario, erosion and deposition rates are equal to or less than the photodecomposition loss rate, with a low rate of surface material cycling. In this case, photodecomposition would remove 2.5 nm yr^{-1} from a bulk carbonate outcrop, but would terminate in the regolith once a carbonate-free lag deposit, equal in thickness to the UV penetration depth, formed. The depth to which a carbonate-free zone would exist in the regolith would depend on the mixing rate and the period of time over which mixing takes place. If the mixing rate equals the maximum photodecomposition rate of 2.5 nm yr^{-1}, the result is a carbonate-free layer 10 meters deep over 4×10^{9} years.

If the effects of mechanical mixing are considered along with erosion, the existence of a carbonate-free zone depends on the relative rates of these processes. The simplest case occurs when the mixing rate at the surface is less than the photodecomposition rate, and the maximum depth of a carbonate free zone will be limited by this rate; for example, a mixing rate of 0.25 nm yr^{-1} would yield over geological time a carbonate-free zone with a maximum depth of 1 meter.

As discussed above however, it is more likely that the surface erosion rate is high relative to any possible photodecomposition rate on Mars, and carbonates would accumulate in the regolith in the absence of mixing. Mechanical mixing of the regolith would cycle this unreacted carbonate back to the surface, resulting in further photodecomposition. In this case, the depth of a carbonate-free region in the regolith will depend on the mixing rate (the rate at which unreacted carbonate is cycled back up to the surface) and the depth of the mixing zone. When the mixing rate exceeds 2.5 nm yr^{-1}, the

carbonate gradient will be zero in mixing zones up to 10 meters deep (i.e. if the mixing zone is 2 meters deep the carbonate-free zone will be 2 meters deep). However, if the depth of the mixing zone exceeds 10 meters, the amount of carbonate moved from the subsurface to the surface will exceed the total load of carbonate that can be decomposed over geological time, resulting in a nonzero gradient of carbonate in the mixing zone. The relationship between photodecomposition and the regolith mixing depth is summarized in Fig. 4.

5. Conclusions

We have seen no evidence of UV-decomposition of $CaCO_3$ when the calcite sample is exposed to UV light in a simulated martian atmosphere at 10 mbar. Based on the experimental lower limit of detection, the upper limit of photodecomposition on Mars is 3.5×10^{-8} molecules/photon. However, it is most likely that UV photodecomposition of $CaCO_3$ does not occur on Mars due to the high pressure of atmospheric CO_2. In vacuum, the decomposition of $CaCO_3$ may occur due to the photodetachment and photodissociation of CO_3^- radical defects generated by UV light. In a CO_2 atmosphere, the decomposition of $CaCO_3$ is suppressed by the reformation of the UV-generated CO_3^- by adsorbed CO_2 and surface O^- radicals.

In the event that photodecomposition is occurring at rates below 3.5×10^{-8} molecules/photon, the depth to which carbonate is decomposed in the regolith will be limited by the rate at which unreacted material is exposed through wind abrasion and the rate at which mechanical mixing of the regolith can cycle carbonates to the surface. Based on our upper limit of photodecomposition on Mars, the maximum depth of a carbonate-free zone in the regolith would be 10 meters. However, assuming the formation of a carbonate-free zone is limited by the photodecomposition rate and not by the erosion rate, the actual depth of the zone will depend on the rate and depth of mechanical mixing of the soil. If the mixing zone is less than 10 meters deep, the depth of the carbonate-free zone will equal the depth of the mixing zone. If the mixing zone depth exceeds ten meters, the amount of carbonate moved to the surface will exceed the total load of carbonate that can be removed from the surface over geological time, resulting in a nonzero gradient which will move carbonate back into the upper ten meters of the regolith.

Acknowledgements

This work was supported by the NASA Exobiology Program (RTOP 344-30-11-02).

References

Bartoll, J., R. Stößer, and M. Nofz 2000. Generation and conversion of electronic defects in calcium carbonates by UV/Vis light. *Appl. Rad. and Isotopes* **52**, 1099-1105.

Blaney, D.L., and T.B. McCord 1990. An observational search for carbonates on Mars. *J. Geophys. Res.* **94**, 10,159-10,166.

Booth, M.C., and H.H. Kieffer 1978. Carbonate formation in Mars-like environments. *J. Geophys. Res.* **83**, 1809-1815.

Calvin, W.M, T.V.V. King, and R. Clark 1994. Hydrous carbonates on Mars?: Evidence from Mariner 6/7 infrared spectrometer and ground-based telescopic spectra. *J. Geophys. Res.* **99**, 14,659-14,675.

Carr, M. H. 1989. Recharge of the early atmosphere of Mars by impact induced release of CO_2. *Icarus* **79**, 311-327.

Carr, M. 1992. Post-Noachian Erosion Rates: Implications for Mars Climate Change. p. 205-206, *LPSC* **23**, 205-206.

Clark, R.N., G.A, Swayze, R.B. Singer, and J. Pollack 1990. High-resolution reflectance spectra of Mars in the 2.3 micrometer region: Evidence for the mineral scapolite. *J. Geophys. Res.* **95**, 14,463-14,480.

Clark, B.C., and D.C. Van Hart 1981. The salts of Mars. *Icarus* **45**, 370-378.

Fanale, F.P., S.E. Postawko, J.B. Pollack, M.H. Carr, and R. O. Pepin 1992. Mars: Epochal climate change and volatile history. In Mars (H.H. Kieffer, B.M. Jakosky, C.W. Snyder, and M.S. Matthews, Eds.), pp. 1135-1179. Univ. of Arizona Press, Tucson.

Fegley, B., and A.H. Treiman 1992. Chemistry of atmosphere-surface interactions on Venus and Mars, Venus and Mars : Atmosphere, Ionospheres, and Solar Wind Interactions, (J.G. Luhmann, M. Tatrallyay, and R. O. Pepin, Eds.), pp. 7-71, AGU, Washington D.C..

Forget, F. and R.T. Pierrehumbert 1997. Warming early Mars with carbon dioxide clouds that scatter infrared radiation. *Science* **278**, 1273-1276.

Gierasch, P.J. and O.B. Toon, 1973. Atmospheric pressure variation and the climate of Mars. *J. Atmos. Sci.* **30**, 1502-1508.

Gooding, J.L. 1978. Chemical weathering on Mars: Thermodynamic stabilities of primary minerals (and their alteration products) from mafic igneous rocks. *Icarus* **33**, 483-513.

Gooding, J.L. 1992. Soil mineralogy and chemistry on Mars: Possible clues from salts and clays in SNC meteorites. *Icarus* **99**, 28-41.

Greeley, R., R.N. Leach, S.H. Williams, B.R. White, J.B. Pollack, D.H. Krinsley, and J.R. Marshall 1982. Rate of Wind Abrasion on Mars. *J. Geophys. Res.*, **87**, 10,009-10,024.

Griffith, L.L. and E.L. Shock, 1995. A geochemical model for the formation of hydrothermal carbonates on Mars. *Nature* **377**, 406-408.

Haberle, R.M., D. Tyler, C.P. McKay, and W.L. Davis 1994. A model for the evolution of CO_2. *Icarus*, **109**, 102-120.

Hiller, J.F., and M.L. Vestal 1980. Tandem quadrupole study of laser photodissociation of CO^-_3. *J. Chem. Phys.*, **72**, 4713-4722.

Hunton, D.E., M. Hofmann, T.G. Lindeman, and A.W. Castleman 1985. Photodissociation dymanics of CO^-_3. *J. Chem. Phys.*, **82**, 134-149.

Jull A.J.T., C.J. Eastoe, S. Xue, and G.F. Herzog 1995. Isotopic composition of carbonates in the SNC meteorites Allan Hills 84001 and Nakla. *Meteoritics* **30**, 311-318.

Kahn, R. 1985. The evolution of CO_2 on Mars, *Icarus* **62**, 175-190.

Kasting, J.F. 1991. CO_2 condensation and the climate of early Mars. *Icarus* **94**, 1- 13.

Khun, W.R., and S.K. Atreya 1979. Solar Radiation Incident on the Martian Surface, *J. Mol. Evol.* **14**, 57-64.

Kirkland, L.E., K.C. Herr, J.W. Salisbury, J.M. McAfee, and P.B. Forney 2001. Determining the TES Detection Limits for Minerals, In *Lunar and Planetary Science XXIX*, Abstract #1864, Lunar and Planetary Institute, Houston (CD-ROM).

McKay, C.P. and W.L. Davis, 1991. Duration of liquid water habitats on early Mars. *Icarus* **90**, 214-221.

McKay, C.P., and S.S. Nedell 1988. Are there carbonate deposits in Valles Marineris, Mars?, *Icarus* **73**, 142-148.

Mischna, M.A., J.F. Casting, A. Pavlov, R. Freeman, 2000. Influnce of carbon dioxide clouds on early martian climate. *Icarus*, **145**, 546-554.

Moseley, J.T., R.A. Bennett, and J.R. Peterson 1974. Photodissociation of CO^{-}_{3}. *Chem. Phys. Letters*, **26**, 2, 288-291.

Mukhin, A.P. Koscheev, Yu. P. Dikov, J. Huth, and H. Wanke 1996. Experimental simulations of the decomposition of carbonates and sulphates on Mars. Nature **379**, 141-143.

O'Connor, J.T. 1968. Mineral stability at the martian surface. *Geophys. Res.* **73**, 5301-5311.

Pollack, J.B., J.F. Kasting, S.M. Richardson, and K. Poliakoff 1987. The case for a wet, warm climate on early Mars. *Icarus* **71**, 203-224.

Pollack, J.B., T. Roush, F. Witteborn, J. Bregman, D. Wooden, C. Stoker, O.B. Toon, D. Rank, B. Dalton, and R. Freedman. 1990. Thermal emission spectra of Mars (5.4 - 10.5 um): Evidence for sulfates, carbonates, and hydrates. *J. Geophys. Res.* **95**, 14,595-14,628.

Roush, T.L., D. Blaney, T.B. McCord, and R. B. Singer 1986. Carbonates on Mars: Searching the Mariner 6 and 7 IRS measurements. In *Lunar and Planetary Science XVII*, pp. 732-733. Lunar and Planetary Institute, Houston.

Schaefer, M.W. 1993. Volcanic recycling of carbonates on Mars. *Geophys. Res. Lett.* **20**, 827-830.

Stoesser, R., J. Bartool, L. Schirrmeister, R.Ernst, and R. Lueck 1996. ESR of trapped holes and electrons in natural and synthetic carbonates, silicates and aluminosilicates. *Appl. Radiat. Isot.* **47**, 1489-1496.

Stern, K.H., and E.L. Weise 1969. High temperature properties and decomposition of inorganic salts, Part 2. Carbonates. *NSRDS-NBS* **30**, p.32.

Stoker, C.R., and M.A. Bullock 1997. Organic degradation under simulated Martian conditions. *J. Geophys. Res.* **102**, 10,881-10,888.

Wright, I.P., M.M. Grady, and C.T. Pillinger 1992. Chassigny and the nakhlites: Carbon-bearing components and their relationship to martian environmental conditions. *Geochim. Cosmochim. Acta* **56**, 817-826.

Table I

Run	Mass Ratio 45/44 ($x10^{-2}$)			Bakeout Temp. (K)	Run Temp. (K)	UV Flux (Photons s^{-1} cm^{-2})	Exposure Time (hours)	LLD Quantum Efficiency (molecules/photon)
	Baseline	LLD	Measured					
A1	1.25	1.32	1.60	293	423	$4.5x10^{17}$	45	$2.6x10^{-7}$*
A3	1.25	1.32	1.34	293	324	$1.3x10^{17}$	48	$2.2x10^{-7}$
A2	1.25	1.32	1.26	293	245	$1.3x10^{17}$	48	$2.2x10^{-7}$
A4	1.25	1.32	1.21	675	325	$1.3X10^{17}$	48	$2.2x10^{-7}$
Blank	1.25	1.32	1.36	293	293	Dark	48	N/A
B1	1.61	1.66	1.61	490	278	$5.4x10^{15}$	11	$2.6x10^{-6}$
B2	1.61	1.66	1.63	490	278	$6.3x10^{16}$	70	$3.5x10^{-8}$
B3	1.61	1.66	1.60	625	278	$8.6x10^{16}$	11	$1.7x10^{-6}$

*Actual calculated quantum efficiency. In all other cases lower limit of detection reported.

Figure 1. Schematic of UV exposure setup. 150W Xe arc lamp(A); IR Filter (B); Nitrogen glove bag (C); Sample cell with sapphire viewport (D); Temperature controlled aluminum block (E); Thermocouple #1 (F); Thermocouple #2 (G); Thermocouple #3 (H). Note that the sketch is not to scale and all samples were illuminated by the beam passing through the IR filter.

Figure 2. Spectral output of Xe lamp used to irradiate samples compared to the radiation incident on the martian surface for 50° N latitude in the spring. Mars spectrum adapted from Khun and Atreya (1979).

Figure 3. Quadrupole Mass Spectrometer (RGA) $^{13}CO_2$ calibration curve.

Figure 4. Weight % of carbonate at the visible surface of the regolith as a function of mixing zone depth for a photodecomposition rate of 2.5 nm yr^{-1}, and erosion rates greater than 2.5 nm yr^{-1}. The initial carbonate content of the soil, due to erosion and mixing: Curve A, 10%; curve B, 3%; curve C, 1%.

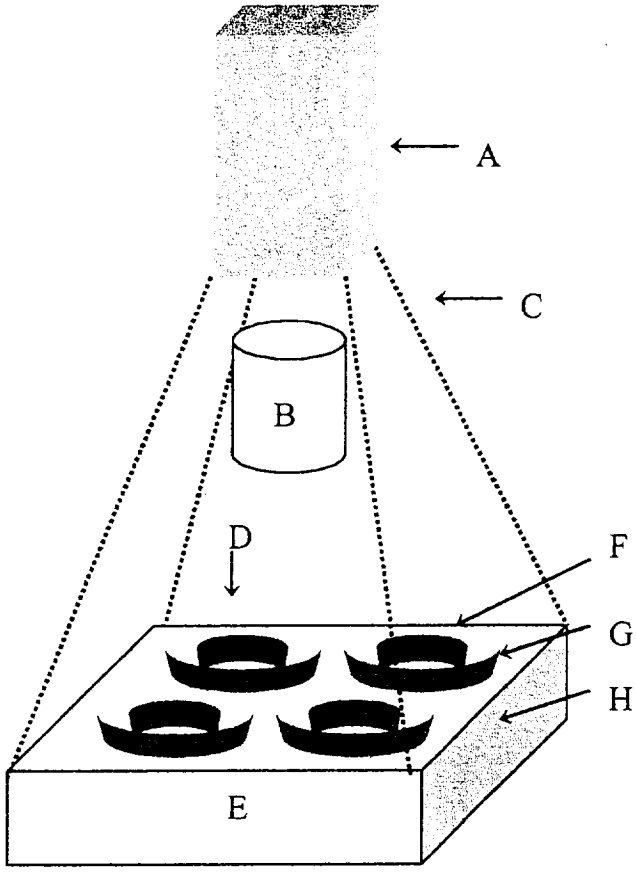

Figure 1

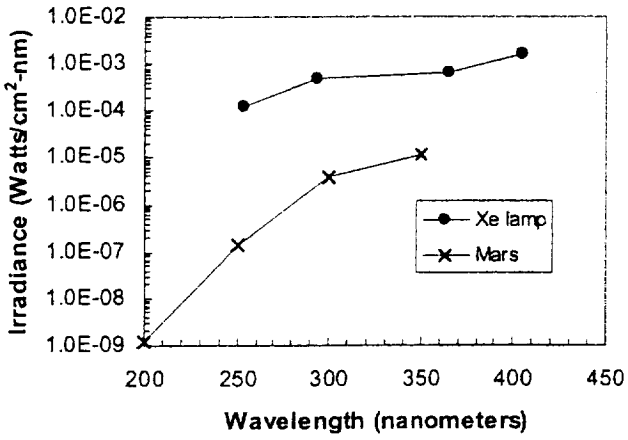
1.0E-02
1.0E-03
1.0E-04
1.0E-05
1.0E-06
1.0E-07
1.0E-08
1.0E-09
Irradiance (Watts/cm²-nm)
200
250
300
350
400
450
Wavelength (nanometers)
Xe lamp
Mars

Figure 2

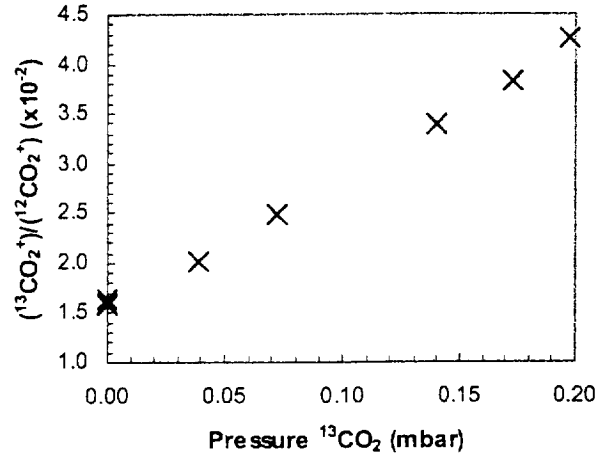
4.5
4.0
3.5
3.0
2.5
2.0
1.5
1.0
0.00
0.05
0.10
0.15
0.20
$(^{13}CO_2^+)/(^{12}CO_2^+)$ $(x10^{-2})$
Pressure $^{13}CO_2$ (mbar)

Figure 3

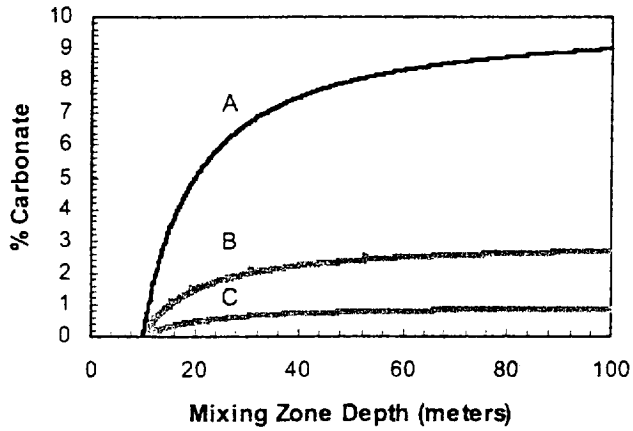
10
9
8
7
6
5
4
3
2
1
0
% Carbonate
A
B
C
0
20
40
60
80
100
Mixing Zone Depth (meters)

Figure 4